

Supporting Information

Revealing the Kinetic Limits of Sodiation and Lithiation at Hard Carbon Using the Diluted Electrode Method

Yuki Fujii,^a Zachary T. Gossage,^a Ryoichi Tatara,^a and Shinichi Komaba^{a,*}

^a *Department of Applied Chemistry, Tokyo University of Science, Shinjuku, Tokyo 162-8601, Japan*

Corresponding Author

* To whom all correspondence should be addressed

E-mail: komaba@rs.tus.ac.jp

Yuki Fujii: <https://orcid.org/0009-0002-8394-8560>

Zachary T. Gossage: <https://orcid.org/0000-0003-3745-2919>

Ryoichi Tatara: <https://orcid.org/0000-0002-8148-5294>

Shinichi Komaba: <https://orcid.org/0000-0002-9757-5905>

Supplemental Figures and Tables

Figure S1. Material characterization: XRD.....	S3
Figure S2. Material characterization: SAXS, Elemental analysis, Particle size distribution.....	S4
Table S1. Mass composition of diluted HC-electrodes.....	S5
Table S3. SEM-EDX images of composite electrodes.....	S6
Figure S4. Electronic conductivity of composite electrodes.....	S7
Figure S5. Capacity correction for rate-capability.....	S8
Table S2. Capacities of diluted HC-electrodes obtained in Na- and Li-cells.....	S9–S10
Figure S6. Rate-capabilities and D_{app} for sodiation and lithiation of HC electrodes.....	S11
Figure S7. Charge-discharge curves during rate-performance testing of 5 vol.% HC-electrode.....	S12
Figure S8. Tafel plots of Na- and Li-cells consisting of 5 vol.% HC-electrode.....	S13
Figure S9. Lithium intercalation into diluted graphite-electrode.....	S14
Figure S10. Rate-capabilities for sodiation and lithiation in ether-based electrolyte.....	S15
Figure S11. Potential-step chronoamperometry for Na-/Li-insertion into diluted HC-electrode.....	S16
Figure S12. Slope- and plateau-capacities obtained by galvanostatic charging.....	S17
Table S3. Characteristic times for sodiation and lithiation of HC.....	S18
Figure S13. Chronoamperograms and D_{app} during sodiation.....	S19
Figure S14. Chronoamperograms and D_{app} during lithiation.....	S20
Figure S15. Electrochemical impedances of Na and Li metal	S21
Figure S16. Nyquist plots of thick 40 vol.% HC-electrode in 3-electrodes cell.....	S22
Figure S17. Bode plots of thick 40 vol.% HC-electrode in 3-electrodes cell.....	S23
Figure S18. Electrochemical impedances of 5 vol.% HC-electrode in Na cell.....	S24
Figure S19. Electrochemical impedances of 5 vol.% HC-electrode in Li cell.....	S25
Figure S20. Equivalent circuits of 5 vol.% HC-electrode in Na- and Li-cell.....	S26
Table S4. Charge-transfer resistances of 5 vol.% HC-electrode in Na- and Li-cell.....	S27
References in supporting information.....	S28

Characteristics of hard carbon

Historically, the HC used in this study was developed for large-scale and high-power lithium-ion batteries, and the attractive property is the smaller surface-area and lower hygroscopic properties. This contributes to less irreversible capacity while maintaining rich alkali-metal storage site like normal commercial HCs.^{1,2}

Characteristics of the hard carbon (HC) powder were investigated by X-ray diffraction, small angle X-ray scattering, elemental analysis, and laser scattering particle-size distribution analysis. The powder XRD pattern was collected using an X-ray diffractometer (SmartLab, Rigaku) in Bragg-Brentano geometry with Ni-filtered Cu K α radiation and a 1D silicon strip detector (D/teX Ultra 250, Rigaku). Small angle X-ray scattering (SAXS) data were collected with the X-ray diffractometer (SmartLab, Rigaku) in a transmission and parallel-beam geometry and a scintillation point detector (SC-70, Rigaku). Elemental composition of HC was evaluated by an organic elemental analyzer (vario EL cube, Elementar). Particle size distribution was evaluated by a laser scattering analyzer (LA-350, HORIBA).

According to the catalog of this HC,² values of BET surface area and true density of HC were 3–7 m² g⁻¹ and 1.52 g cm⁻³, respectively. Obtained values of d_{002} and L_a were almost consisted with catalog of this HC.² The graphitization degree estimated from 10 and 11 diffraction profiles were 0.09 and 0.15, respectively. However, further refinement is required to ensure the accuracy of graphitization degree. The micropore size, 1.05 nm, is consistent with that of sucrose-derived HC synthesized at 1300 °C,³ and it may result in pseudo-metallic cluster with 2–4 atoms both of sodium and lithium storage. Existence of sulfur in low elemental compositions may be attributed to the petroleum pitch used as raw material.² Values of D_{50} and standard error of particle size distribution were 9.0 μ m and 3.5 μ m, respectively, and they were well consisted with previous reports.^{1,2}

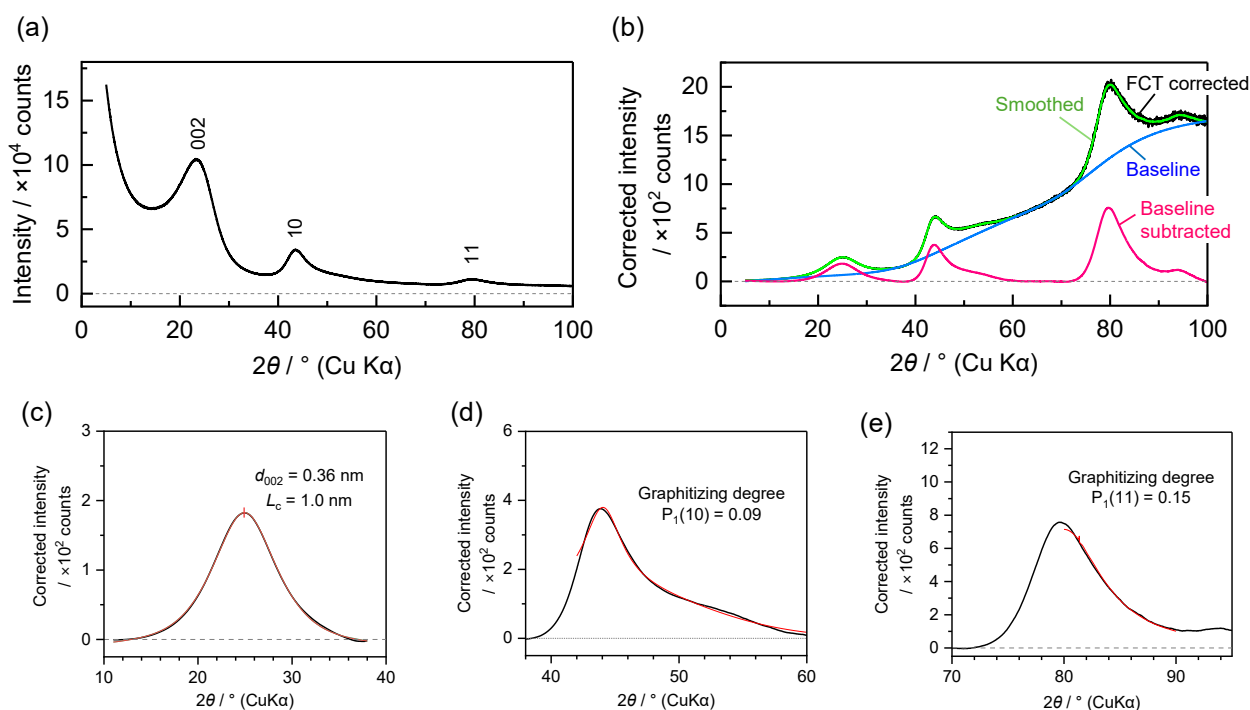
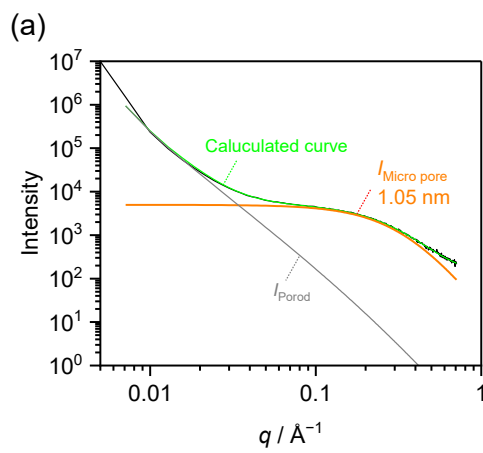


Figure S1. X-ray diffraction patterns (a) as measured, (b) corrected by FCT factors and baseline subtraction, (c) 002 diffraction peak fitted by using pseudo-Voigt function to estimate values of d_{002} and L_c . (d) 10 and (e) 11 diffraction peak fitted by using turbostratic stacking proposed by Fujimoto⁴ to evaluate graphitizing degree. All fittings were performed with non-linear fitting in OriginPro software.



(b)

Element	Ratio / wt. %	Ratio to C
C	95.37	-
H	0.56	0.006
N	0.22	0.002
S	1.08	0.011

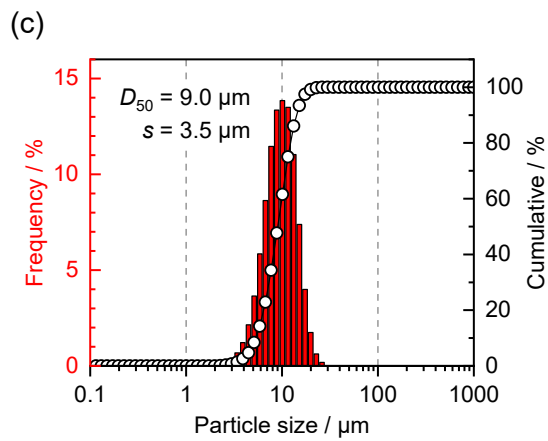
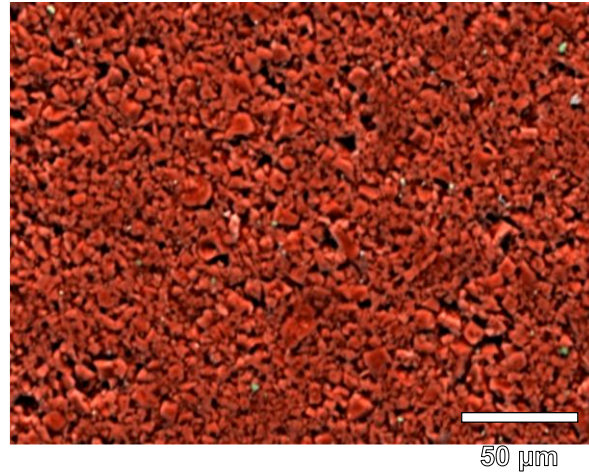


Figure S2. (a) Small angle X-ray scattering patterns and calculation line fitted by using NANO-Solver (Rigaku), (b) elemental composition and (c) particle-size distribution of the HC powders.

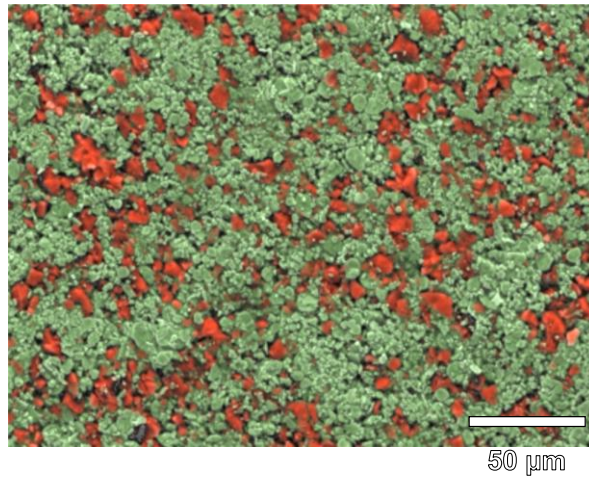
Table S1. Mass compositions of diluted HC-electrodes.

HC-concentration	HC / mg	Al ₂ O ₃ / mg	PANa / mg	SWCNT(Lamfil) / mg	CMC (Lamfil) / mg
95 vol.%	72.20	0	3.25	0.4	0.6
40 vol.%	30.40	109.18	3.25	0.4	0.6
10 vol.%	7.60	168.73	3.25	0.4	0.6
5 vol.%	3.80	178.65	3.25	0.4	0.6
2 vol.%	1.52	184.61	3.25	0.4	0.6

(a) 95 vol.% HC



(b) 40 vol.% HC



(c) 5 vol.%

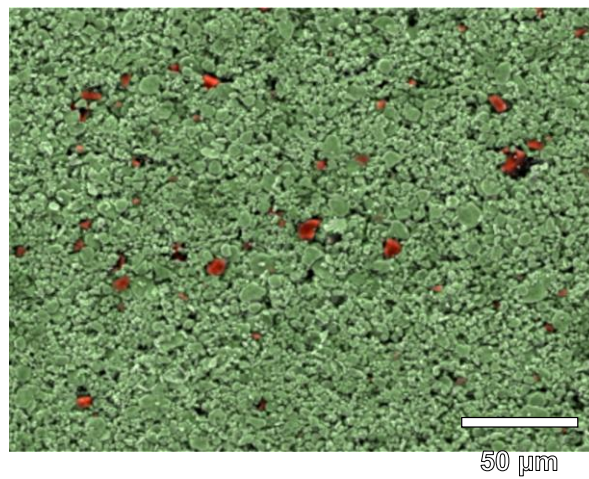


Figure S3. Images of SEM-EDX mapping of diluted electrodes with lower magnification. HC loadings were (a)95, (b)40, and (c) 5 vol.% of electrode volume. C and Al element were highlighted with red and green, respectively.

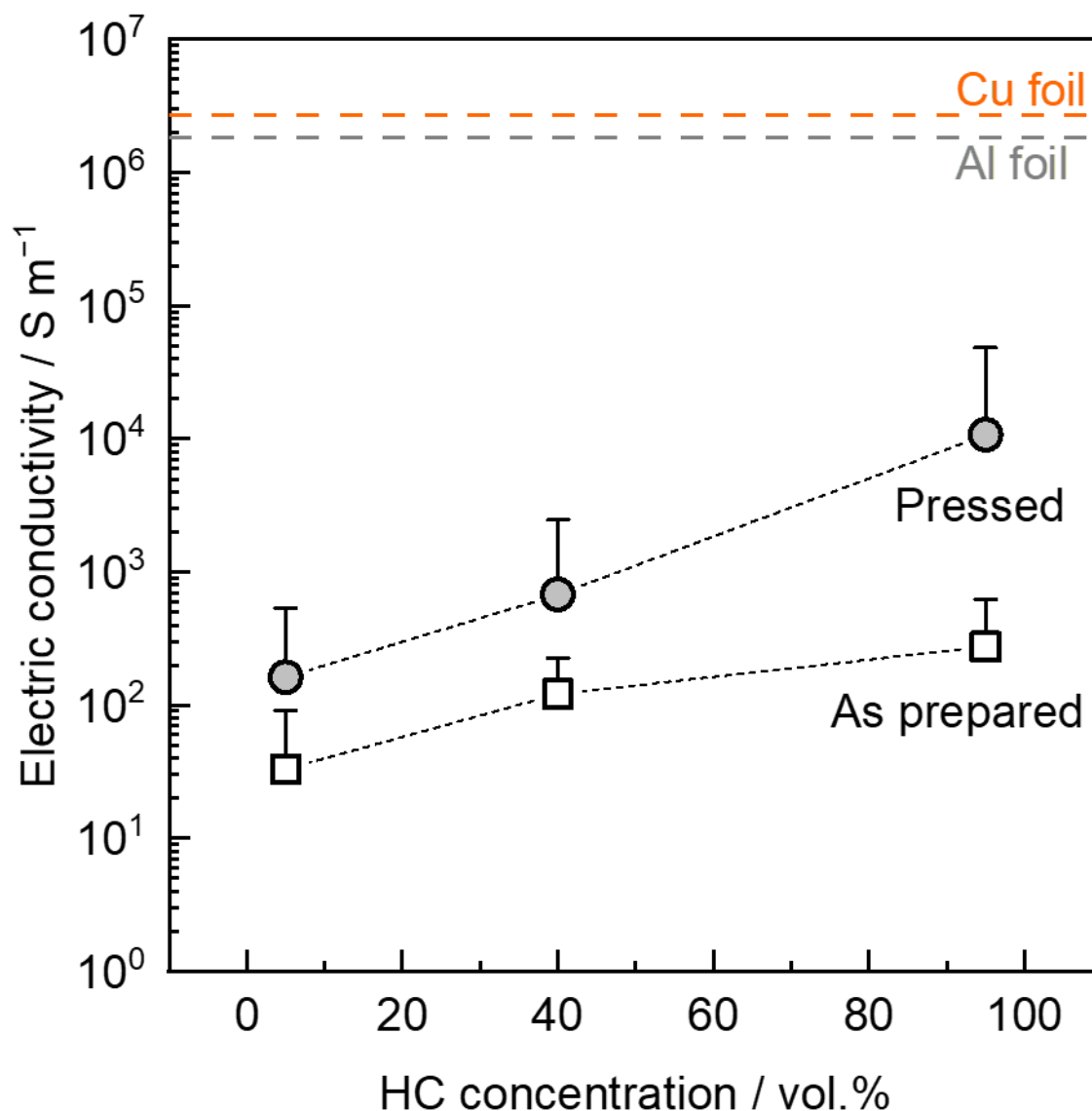


Figure S4. In-plane electronic conductivity of (un)diluted HC-electrodes. The values of electronic conductivity were calculated from resistance measured by a resistivity meter Loresta-GX (MCP-T700, Mitsubishi chemical analytech) with a PSP probe (RMH112, 1.5 mm pins-distance). Error bars show variety of electronic conductivity across an electrode sheet. Electrode pressing was performed prior to analysis by a single-axis press with ~100 MPa.

Capacity correction for rate-capability

Capacity of SWCNT was estimated by eqn (S1) generated from rate-capability of 0 vol.% HC-electrode (95 vol.% Al₂O₃-electrode)

$$Q_{\text{SWCNT}}[\text{mAh cm}_{(\text{WE})}^{-3}] = A1 \exp\left(-\frac{i}{t1}\right) + A2 \exp\left(-\frac{i}{t2}\right) + A3 \exp\left(-\frac{i}{t3}\right) + y0 \quad (\text{S1})$$

Q_{SWCNT} values for each cycle of diluted HC-electrode were estimated by using 0 vol.% HC-electrodes, which contained the same loading of SWCNT in the unit volume of composite electrode (Fig. S5a and b). Q_{HC} can be evaluated from eqn (S2) as a corrected capacity:

$$Q_{\text{HC}}[\text{mAh g}_{(\text{HC})}^{-1}] = (q_{\text{WE}} - Q_{\text{SWCNT}} \times V_{\text{composite electrode}} \times i_{\text{Reduction}}) / m_{\text{HC}} \quad (\text{S2})$$

Here, q_{WE} and $i_{\text{Reduction}}$ are the actual capacities [mAh] and the applied current [A] for electrochemical reduction during rate capability test, respectively. $V_{\text{composite electrode}}$ is volume of composite electrode which was evaluated by using thickness measured with a dial gauge (ID-S1012B, Mitsutoyo) and diameter of working electrode, i.e., 10 mm. m_{HC} is the mass of HC loaded in diluted electrode.

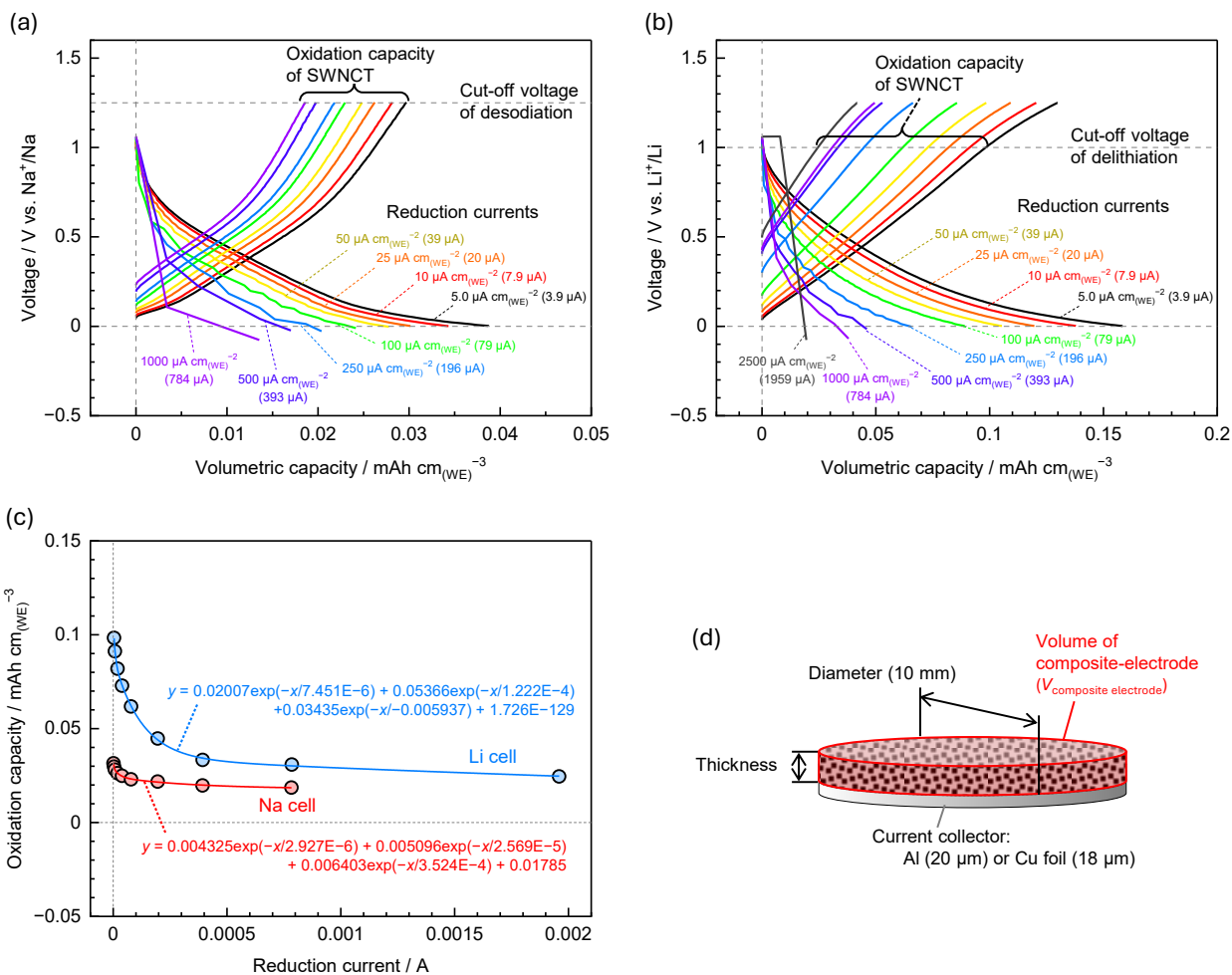


Figure S5. Charge/discharge curves of 0 vol.% HC-electrodes during rate-capability test for electrochemical reduction in (a) Na- and (b) Li-cell. (c) Rate capability of volumetric capacity as function of applied reduction current. (d) Schematic illustration of $V_{\text{composite electrode}}$.

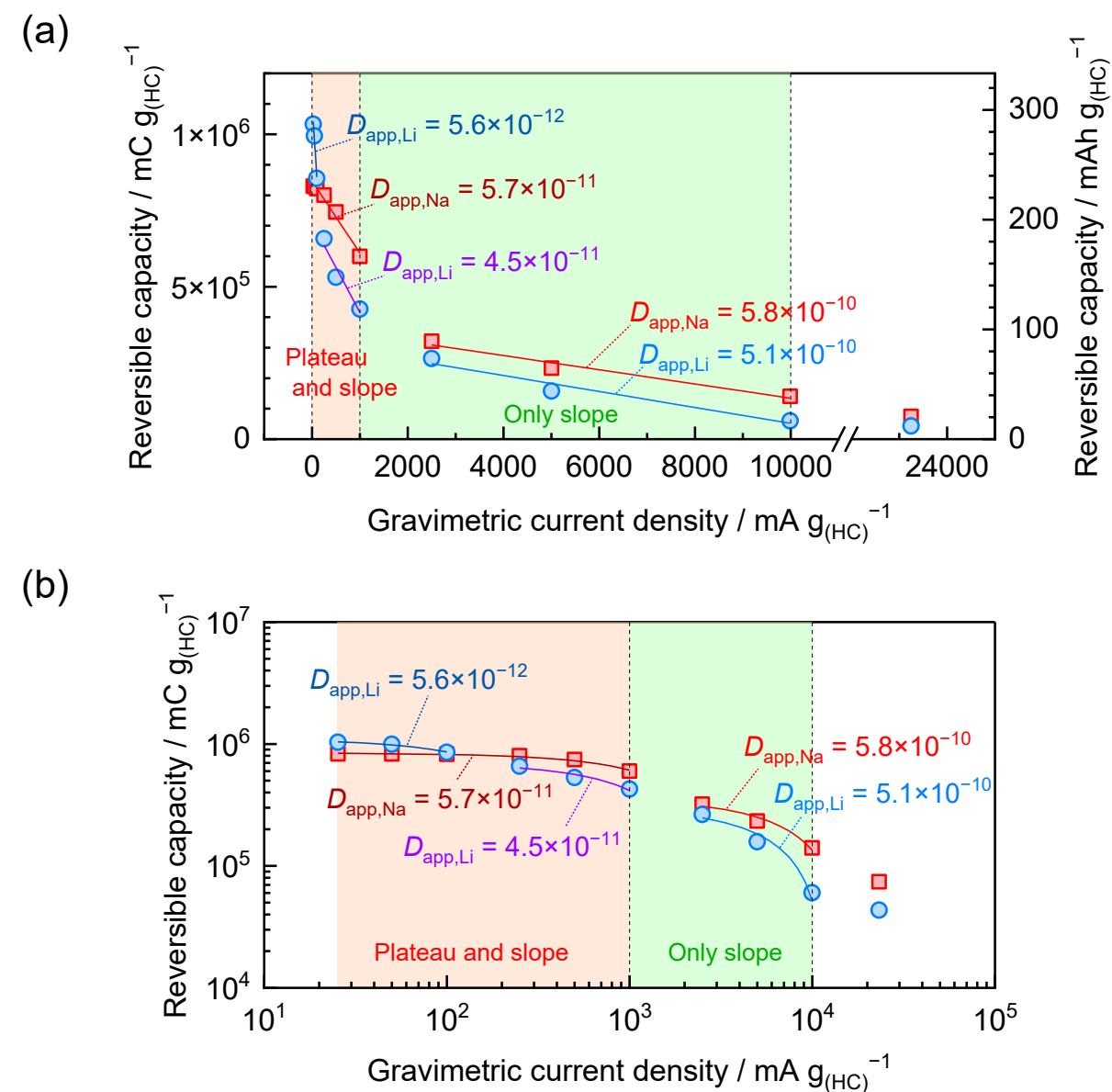
Table S2. Capacities of diluted HC-electrodes obtained in Na- and Li-cells.

Na 95 vol.%						Li 95 vol.%					
(Thickness = 47.4 μm , Volume = $3.72 \times 10^{-3} \text{ cm}^3$, HC mass = 3.51 mg)						(Thickness = 40.2 μm , Volume = $3.16 \times 10^{-3} \text{ cm}^3$, HC mass = 3.05 mg)					
Current / mA g _(HC) ⁻¹	WE / mAh	SWCNT / mAh	Subtracted / mAh	HC / mAh g _(HC) ⁻¹	Normalized / %	Current / mA g _(HC) ⁻¹	WE / mAh	SWCNT / mAh	Subtracted / mAh	HC / mAh g _(HC) ⁻¹	Normalized / %
21.74	0.8175	8.504E-4	0.8223	234.3	100.4	10	0.8726	0.00241	0.8702	285.3	103.9
22.36	0.8185	8.484E-4	0.8238	234.7	100.5	25.75	0.8395	0.001961	0.8376	274.6	100
25.02	0.8141	8.399E-4	0.8206	233.8	100	50.16	0.7332	0.001542	0.7317	239.9	87.36
50.11	0.6211	7.669E-4	0.6068	172.9	76.28	64.26	0.6561	0.00139	0.6547	214.7	78.17
55.78	0.5704	7.521E-4	0.5696	162.3	70.04	128.9	0.5369	0.001083	0.5359	175.7	63.98
112	0.3397	6.343E-4	0.3411	97.19	41.68	257.5	0.465	9.53E-4	0.464	152.1	55.4
223.7	0.2926	5.035E-4	0.2914	83.02	35.89	642.6	0.3672	7.796E-4	0.3664	120.1	43.74
558.1	0.2474	4.068E-4	0.245	69.79	30.34	1289	0.2714	5.594E-4	0.2708	88.8	32.34
1119	0.141	3.974E-4	0.1388	39.53	17.25	2575	0.1517	2.89E-4	0.1514	49.65	18.08
2236	0.0598	3.972E-4	0.0552	15.73	7.271						

Na 40 vol.%						Li 40 vol.%					
(Thickness = 42.6 μm , Volume = $3.35 \times 10^{-3} \text{ cm}^3$, HC mass = 1.21 mg)						(Thickness = 41.8 μm , Volume = $3.28 \times 10^{-3} \text{ cm}^3$, HC mass = 1.23 mg)					
Current / mA g _(HC) ⁻¹	WE / mAh	SWCNT / mAh	Subtracted / mAh	HC / mAh g _(HC) ⁻¹	Normalized / %	Current / mA g _(HC) ⁻¹	WE / mAh	SWCNT / mAh	Subtracted / mAh	HC / mAh g _(HC) ⁻¹	Normalized / %
16.2	0.2906	8.163E-4	0.2929	242	101.1	12.2	0.3839	0.002771	0.3811	309.8	107.9
25.05	0.2875	8.046E-4	0.289	238.8	100	24.4	0.3556	0.002512	0.3531	287	100
32.49	0.2853	7.964E-4	0.2861	236.5	99.25	48.79	0.3099	0.002195	0.3077	250.2	87.15
50.1	0.2803	7.776E-4	0.2808	232.1	97.53	122	0.2467	0.001616	0.2451	199.2	69.42
64.89	0.274	7.625E-4	0.2744	226.8	95.33	244	0.2049	0.001223	0.2037	165.6	57.7
161.9	0.2288	6.759E-4	0.2289	189.1	79.57	487.9	0.1749	0.001032	0.1739	141.4	49.25
324.8	0.1405	5.701E-4	0.1398	115.6	48.8	1220	0.1401	8.758E-4	0.1392	113.2	39.43
648.8	0.0993	4.526E-4	0.09855	81.44	34.43	2440	0.1103	6.803E-4	0.1096	89.1	31.04
1619	0.0739	3.656E-4	0.07223	59.7	25.57	4878	0.07562	4.105E-4	0.07521	61.15	21.3
3248	0.0463	3.571E-4	0.04384	36.23	15.95						
6488	0.0152	3.57E-4	0.01054	8.713	5.095						

Na 10 vol.% (Thickness = 42 μm , Volume = $3.30 \times 10^{-3} \text{ cm}^3$, HC mass = 0.29 mg)						Li 10 vol.% (Thickness = 40.6 μm , Volume = $3.19 \times 10^{-3} \text{ cm}^3$, HC mass = 0.31 mg)					
Current / $\text{mA g}_{\text{HC}}^{-1}$	WE / mAh	SWCNT / mAh	Subtracted / mAh	HC / $\text{mAh g}_{\text{HC}}^{-1}$	Normalized / %	Current / $\text{mA g}_{\text{HC}}^{-1}$	WE / mAh	SWCNT / mAh	Subtracted / mAh	HC / $\text{mAh g}_{\text{HC}}^{-1}$	Normalized / %
25.18	0.0698	8.814E-4	0.07222	249	100	24.93	0.0976	0.002933	0.09467	310.4	100
27.25	0.0699	8.701E-4	0.07153	246.7	100.2	49.84	0.0968	0.002687	0.09411	308.6	99.39
49.97	0.0696	8.16E-4	0.07018	242	99.78	64.3	0.09187	0.002595	0.08927	292.7	94.24
67.55	0.06938	8.049E-4	0.0697	240.3	99.48	100	0.0835	0.002434	0.08107	265.8	85.56
135.6	0.0685	7.851E-4	0.06861	236.6	98.29	128.9	0.0772	0.002332	0.07487	245.5	78.99
270.8	0.0663	7.517E-4	0.06625	228.4	95.16	257.6	0.0644	0.001981	0.06242	204.7	65.79
675.5	0.0565	6.664E-4	0.05623	193.9	81.01	643.3	0.0496	0.001403	0.0482	158	50.67
1356	0.03722	5.62E-4	0.03674	126.7	53.09	1290	0.0394	0.001094	0.03831	125.6	40.19
2708	0.0244	4.461E-4	0.02355	81.22	34.54	2576	0.029	9.623E-4	0.02804	91.93	29.28
6755	0.0162	3.605E-4	0.01484	51.17	22.67	6439	0.015	7.869E-4	0.01421	46.6	14.57
1.356E4	0.00829	3.521E-4	0.006198	21.37	11.18	1.29E4	0.0076	5.646E-4	0.007035	23.07	7.048

Na 5 vol.% (Thickness = 42 μm , Volume = $3.30 \times 10^{-3} \text{ cm}^3$, HC mass = 0.15 mg)						Li 5 vol.% (Thickness = 41.8 μm , Volume = $3.28 \times 10^{-3} \text{ cm}^3$, HC mass = 0.15 mg)					
Current / $\text{mA g}_{\text{HC}}^{-1}$	WE / mAh	SWCNT / mAh	Subtracted / mAh	HC / $\text{mAh g}_{\text{HC}}^{-1}$	Normalized / %	Current / $\text{mA g}_{\text{HC}}^{-1}$	WE / mAh	SWCNT / mAh	Subtracted / mAh	HC / $\text{mAh g}_{\text{HC}}^{-1}$	Normalized / %
25.34	0.03557	0.001004	0.03598	239.9	100	25.34	0.04716	0.00323	0.04393	292.9	100
50.01	0.03549	8.774E-4	0.0353	235.3	99.91	50.01	0.04541	0.003024	0.04239	282.6	96.48
100	0.03515	8.143E-4	0.03487	232.5	99.07	100	0.0394	0.002771	0.03663	244.2	83.37
250.1	0.03416	7.868E-4	0.03383	225.5	96.39	250.1	0.03067	0.002421	0.02825	188.3	64.29
500.1	0.03183	7.546E-4	0.03144	209.6	89.8	500.1	0.02496	0.002067	0.0229	152.6	52.11
999.3	0.02571	6.974E-4	0.02512	167.5	72.24	999.3	0.02012	0.001616	0.01851	123.4	42.12
2501	0.01403	5.699E-4	0.0133	88.68	38.67	2501	0.01281	0.001141	0.01167	77.78	26.56
5002	0.01033	4.531E-4	0.009393	62.62	28.08	5002	0.008185	9.977E-4	0.007187	47.92	16.36
9987	0.006446	3.739E-4	0.004901	32.68	16.93	9987	0.003969	8.763E-4	0.003093	20.62	7.041
2.325E4	0.003678	3.523E-4	0.001626	10.84	8.931	2.325E4	0.002914	6.268E-4	0.002287	15.25	5.206



(c)

Sodiation		Lithiation	
Current / mA g _(HC) ⁻¹	D_{app} (\pm Error) / cm ² s ⁻¹	Current / mA g _(HC) ⁻¹	D_{app} (\pm Error) / cm ² s ⁻¹
25–1000	5.7×10^{-11} ($\pm 3.1 \times 10^{-11}$)	25–100	5.6×10^{-12} ($\pm 3.1 \times 10^{-10}$)
		250–1000	4.5×10^{-11} ($\pm 2.5 \times 10^{-11}$)
2500–10000	5.8×10^{-10} ($\pm 3.2 \times 10^{-10}$)	2500–10000	5.1×10^{-10} ($\pm 2.8 \times 10^{-10}$)

Figure S6. Rate-capabilities and D_{app} for Na- and Li-insertion of 5 vol.% HC-electrodes with horizontal axis of current in (a) linear and (b) logarithm. D_{app} was estimated by eqn (1) in main text using slope in (a). (c) Summary of D_{app} values with error attributed to the particle size distribution of HC.

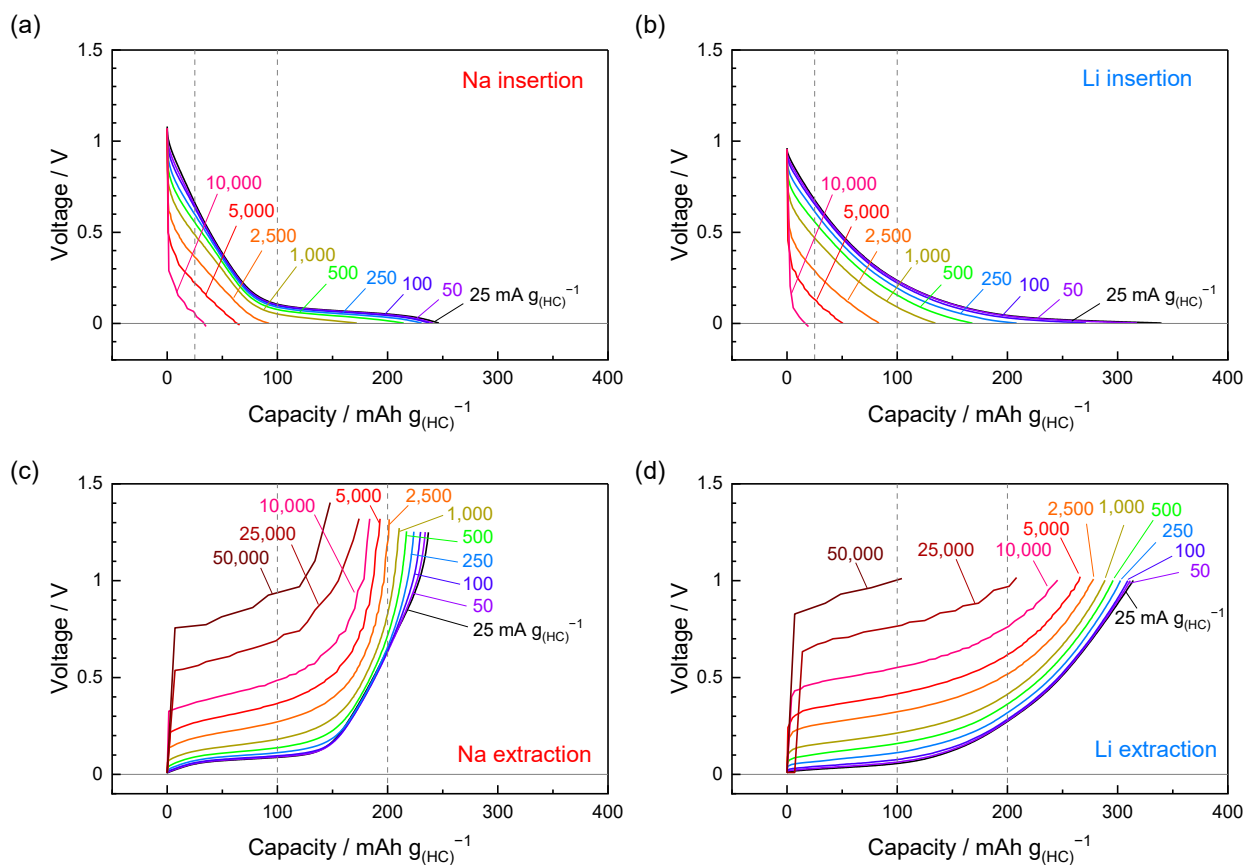


Figure S7. Galvanostatic charge-discharge curves during rate-performance testing of 5 vol.% HC-electrode in Na- and Li-cell. Tests were performed for (a) sodiation, (b) lithiation, (c) desodiation, and (d) delithiation, respectively. The applied current for opposite process was fixed to 25 mA g^{-1} in each test.

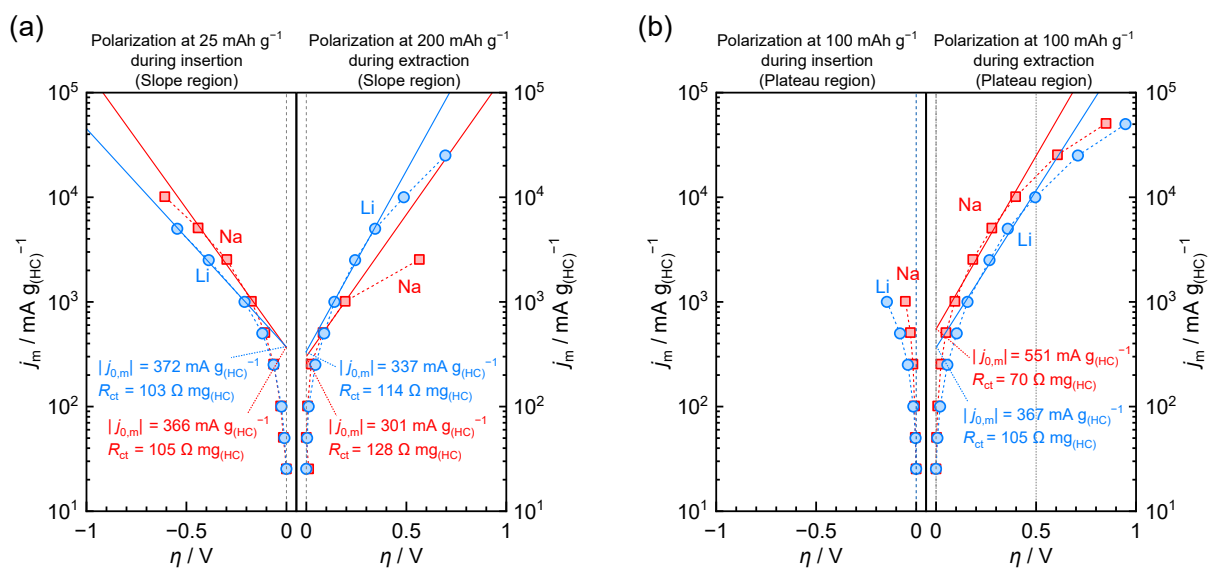


Figure S8. Tafel plots prepared by using polarization at (a) slope region at 25 mA h⁻¹ during insertion and 200 mA h⁻¹ during extraction and (b) plateau region at 100 mA h⁻¹ during insertion and 100 mA h⁻¹ during extraction in Fig. S2. The plot of Na-cell (□) and Li-cell (○) were obtained by voltage-subtraction from charge-discharge curves at lower currents.

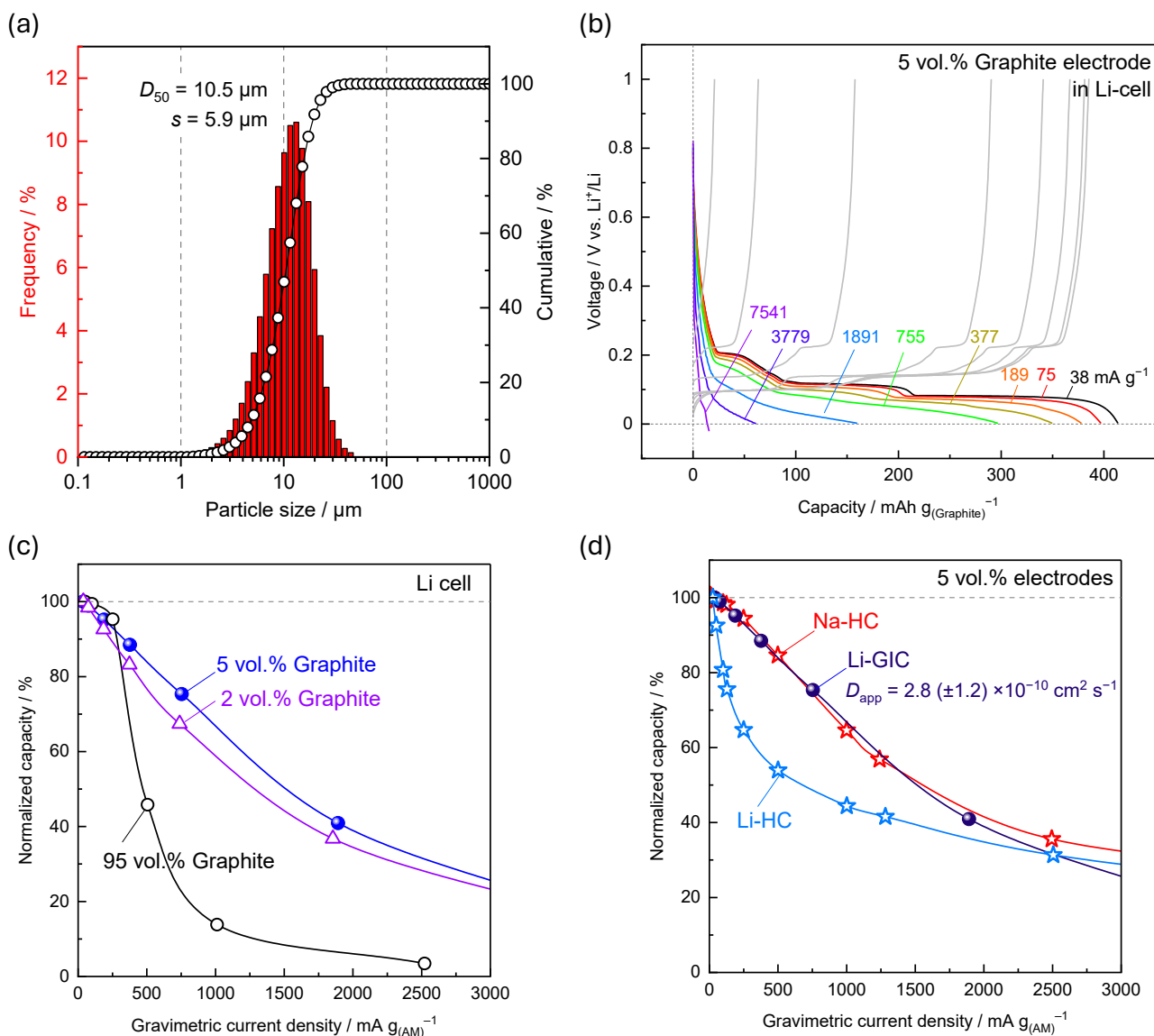


Figure S9. Lithium intercalation into diluted graphite-electrodes in Li-half cell using conventional electrolyte, 1 M LiPF₆ EC:DMC (1:1 v/v) with 2 vol.% adding fluoroethylene carbonate (FEC). (a) Particle size distribution of the graphite powder. (b) Galvanostatic charge-discharge curves of 5 vol.% graphite-electrode during rate-capability testing for lithium-intercalation. (c) Rate-capabilities of diluted electrodes having various graphite concentrations. (d) Rate-capabilities of Na-/Li-insertion into 5 vol.% HC-electrodes and Li-intercalation into 5 vol.% graphite-electrodes.

Relating to the diffusion dimensionality, eqn (1) for estimation of D_{app} was slightly change as eqn (S3):⁵

$$Q = \frac{Ca}{3} - \frac{a^2}{8D_{app}} j_m \quad (S3)$$

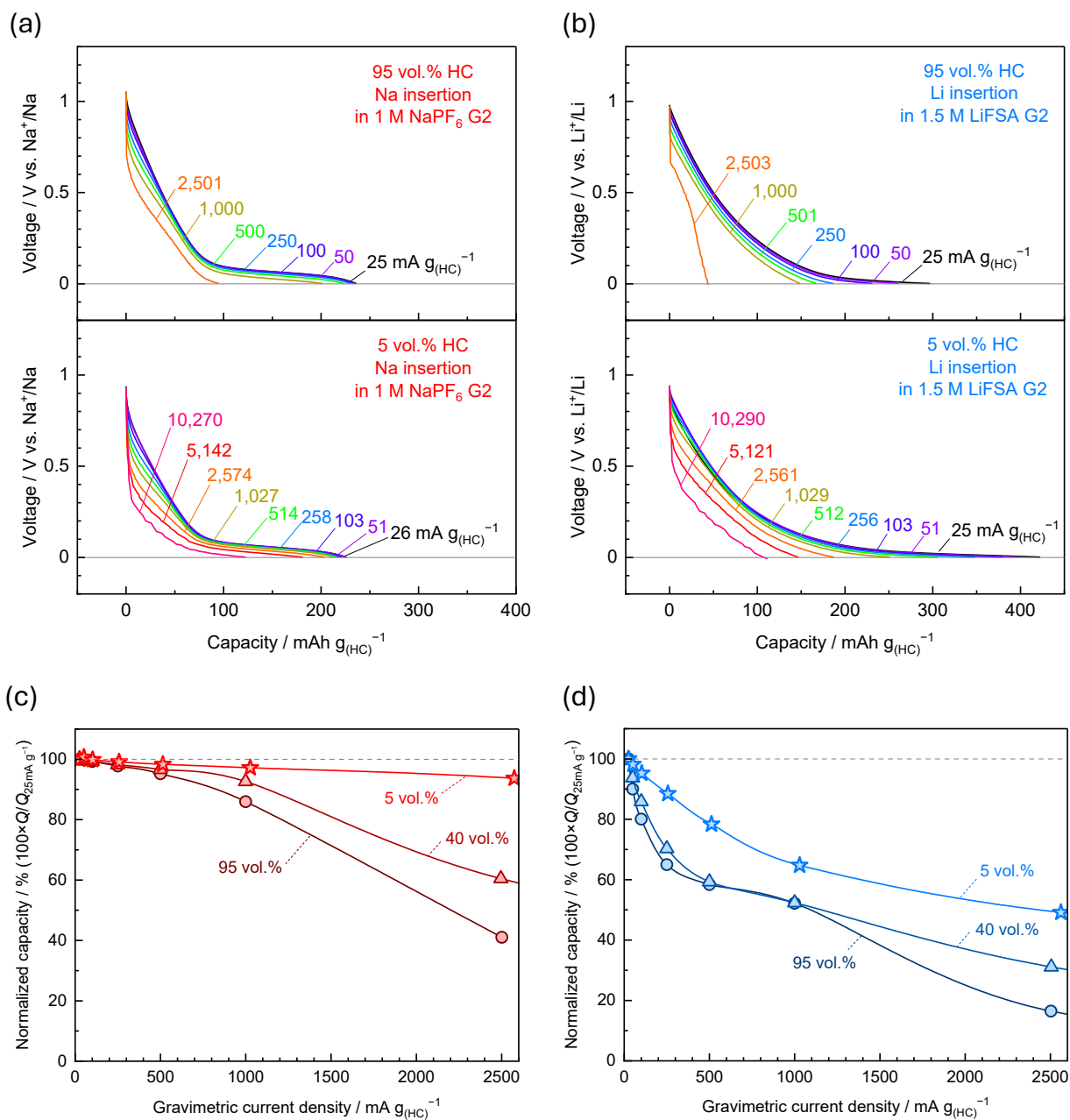


Figure S10. Rate capability test in ether-based electrolyte. Sodiation/lithiation curves of HC electrodes in (a) Na-cells with 1 M NaPF_6 in G2 and (b) Li-cells with 1.5 M lithium bis(fluorosulfonyl)amide in G2, respectively. Rate capabilities of (c) sodiation and (d) lithiation as a function of applied current.

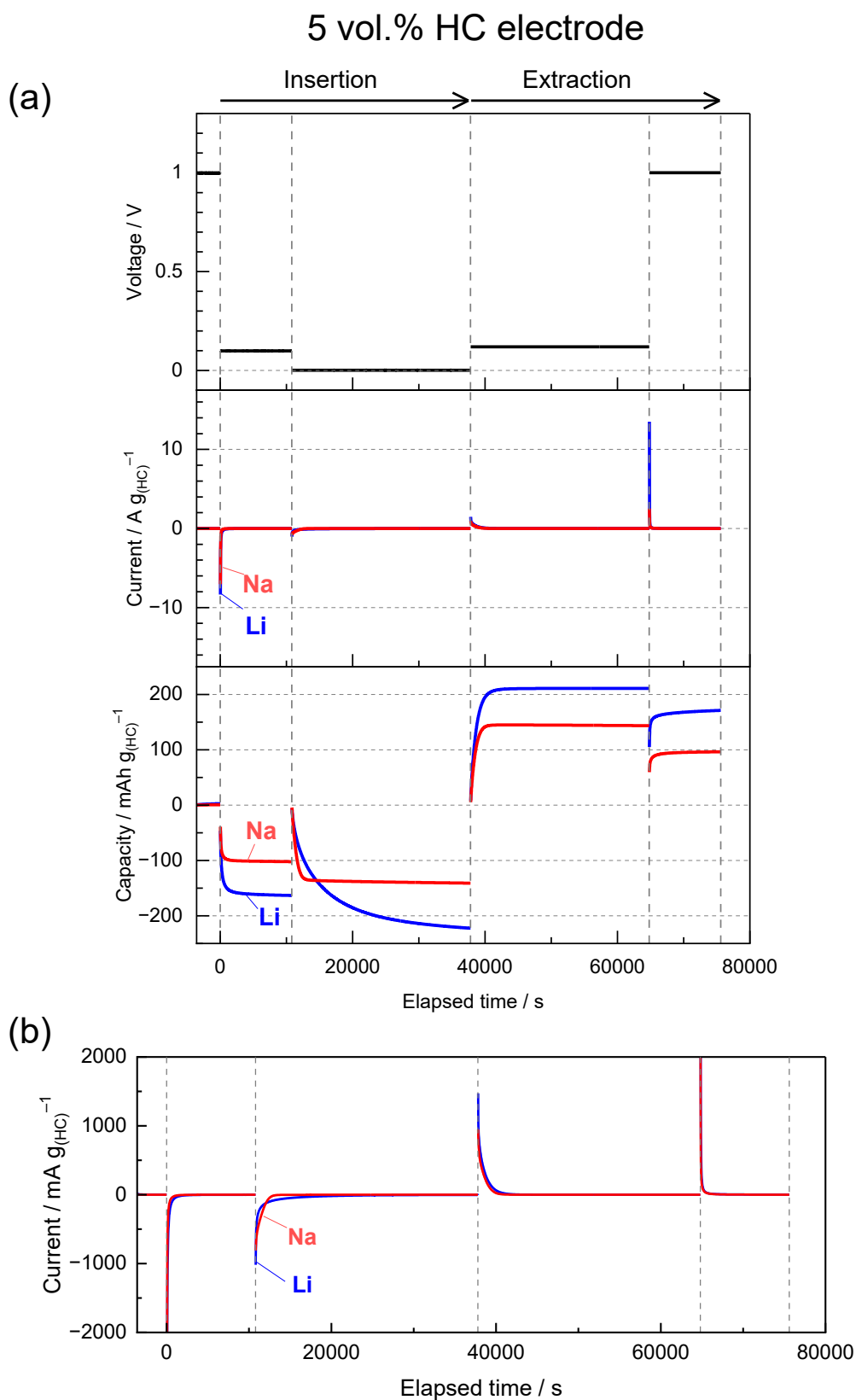


Figure S11. PSCA result of 5 vol.% HC-electrode in Na- and Li-cell. (a) Potential, current, and capacity were shown in top, middle, and bottom panel in the above graph, respectively. (b) Magnified current from (a) to compare at long times of 15000–60000 s.

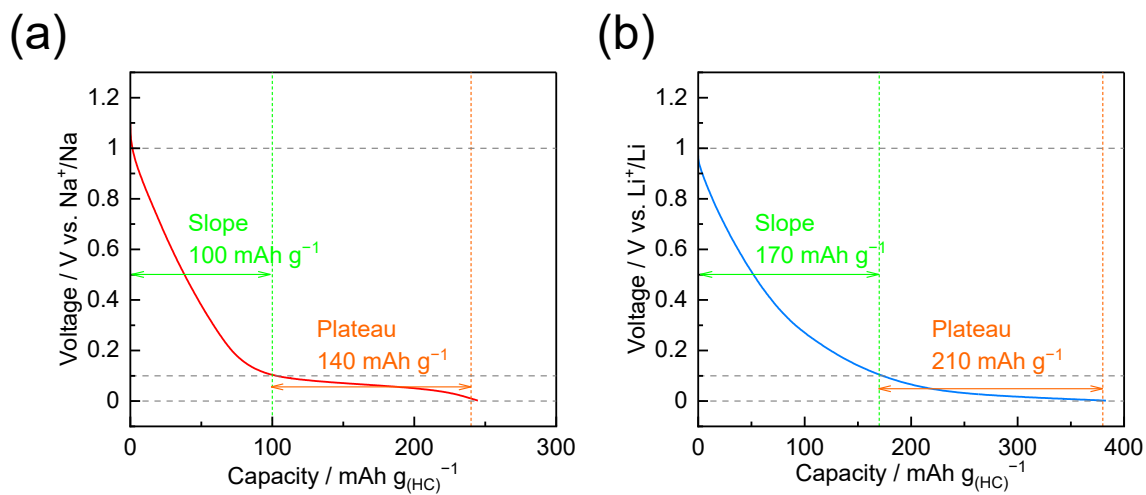


Figure S12. Slope- and plateau-capacity of HC during galvanostatic charge-discharge, Q_{GCD} , in (a) Na- and (b) Li-cell at 25 mA g^{-1} . Slope capacity was defined between 1.0 V and 0.1 V, and the plateau capacity was defined between 0.1 V and 2 mV.

Table S3. Characteristic time, Tau (τ) from the chronocoulogram of 5 vol.% HC-electrode in Na- and Li-cells. τ is evaluated from the time at which the cell reaches 63.2 % of the slope-/plateau-capacity.

Temperature / °C	$\tau_{\text{Na,slope}} / \text{S}$	$\tau_{\text{Na,plateau}} / \text{S}$	$\tau_{\text{Li,slope}} / \text{S}$	$\tau_{\text{Li,plateau}} / \text{S}$
40	24	206	56	1013
30	50	433	113	2157
25	63	677	169	3499
20	87	953	257	5419
10	244	1817	812	14760

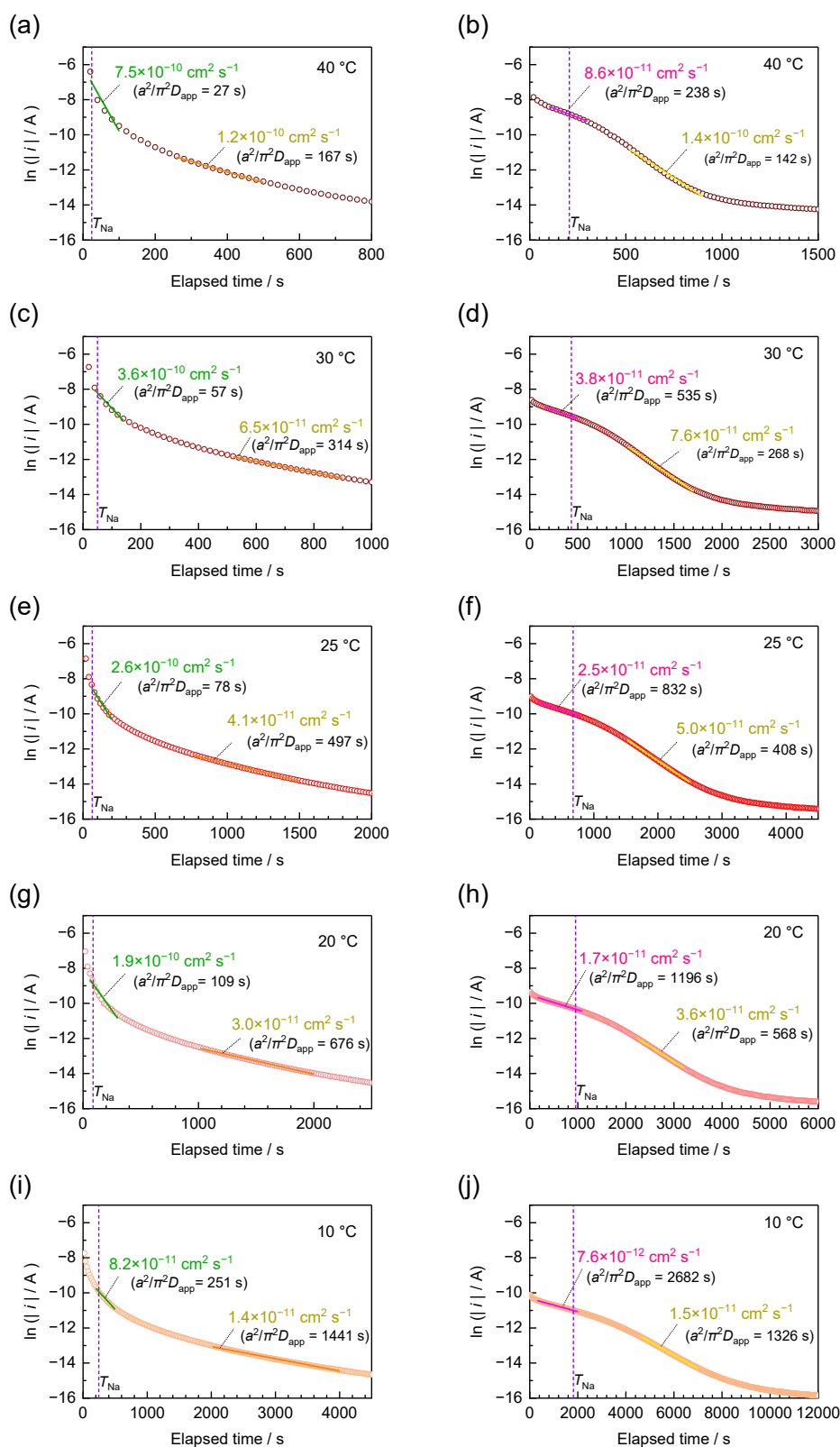


Figure S13. Chronoamperograms during sodiation in 5 vol.% electrodes. Potential step for slope region (from 1.0 V to 0.1 V) and plateau region (from 0.1 V to 2 mV) were carried out, sequentially at (a)-(b) 40 °C, (c)-(d) 30 °C, (e)-(f) 25 °C, (g)-(h) 20 °C, and (i)-(j) 10 °C, respectively. D_{app} were estimated using two time-regions, one near the τ_{Na} shown in Table S4 and the other after the diffusion characteristic time, $a^2/\pi^2 D_{app}$. These are referred to as $D_{app,\tau}$ and $D_{app,late}$ in the main text.

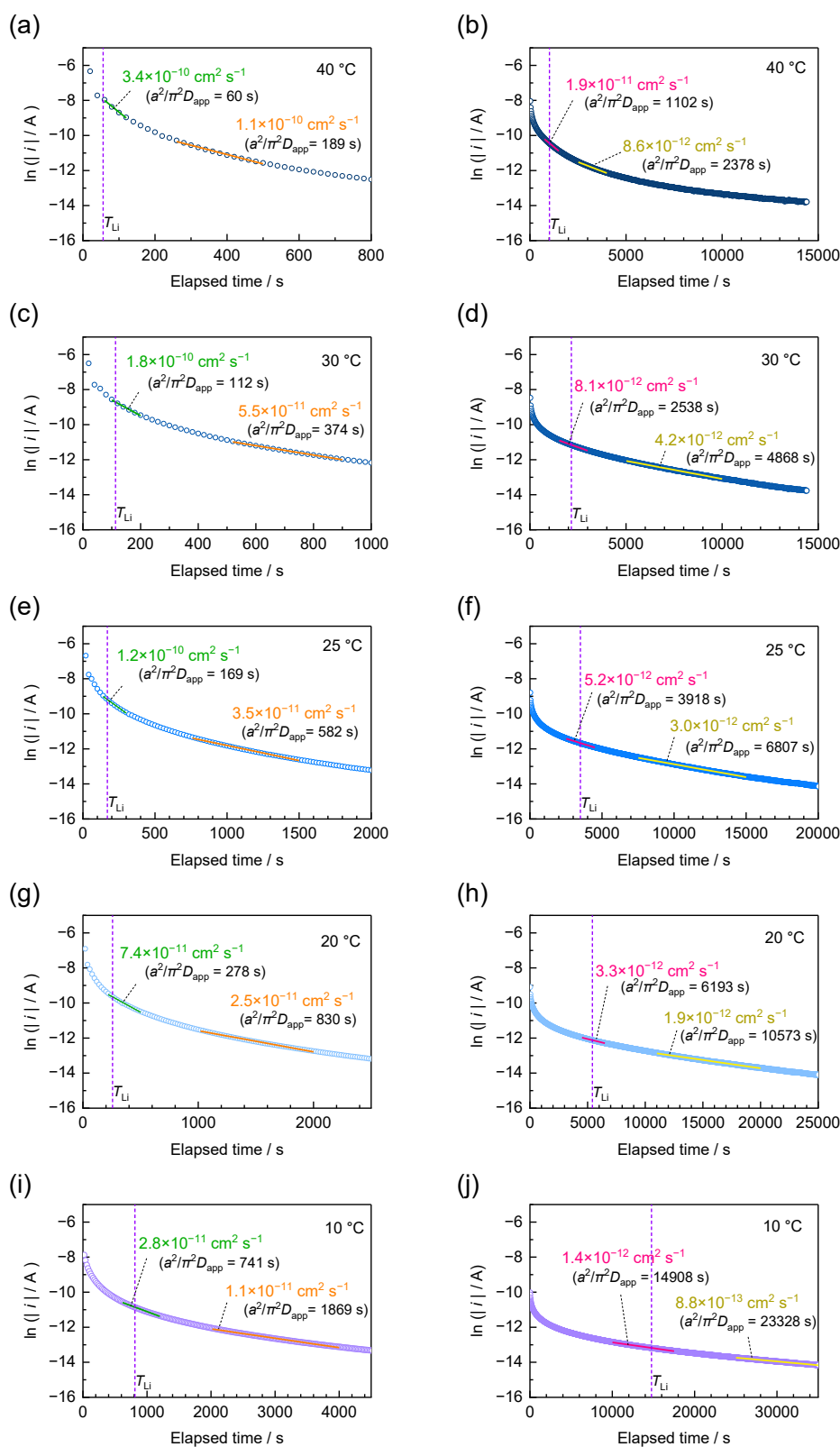


Figure S14. Chronoamperograms during lithiation in 5 vol.% electrode. Potential step for slope region (from 1.0 V to 0.1 V) and plateau region (from 0.1 V to 2 mV) were carried out, sequentially at (a)-(b) 40 °C, (c)-(d) 30 °C, (e)-(f) 25 °C, (g)-(h) 20 °C, and (i)-(j) 10 °C, respectively. D_{app} were estimated using two time-regions with one near the τ_{Li} shown in Table S4 and the other after diffusion characteristic time, $a^2/\pi^2 D_{app}$. These are referred to as $D_{app,\tau}$ and $D_{app,late}$ in the manuscript.

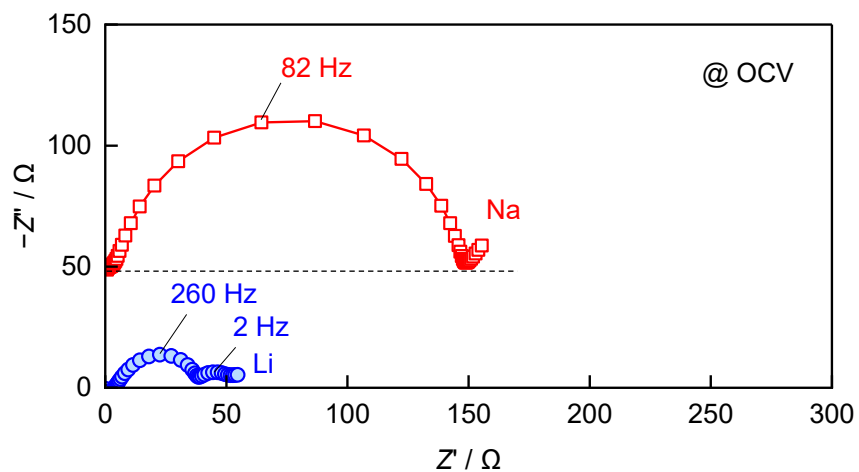


Figure S15. Nyquist plots of electrochemical impedance of Na and Li metal electrodes. These impedances were obtained by dividing Z' and $-Z''$ of Na//Na cell and Li//Li cell by 2, respectively, to compare with half-cells consisting of HC-electrode. Nyquist plots of Na have been vertically shifted to 50 Ω for visibility.

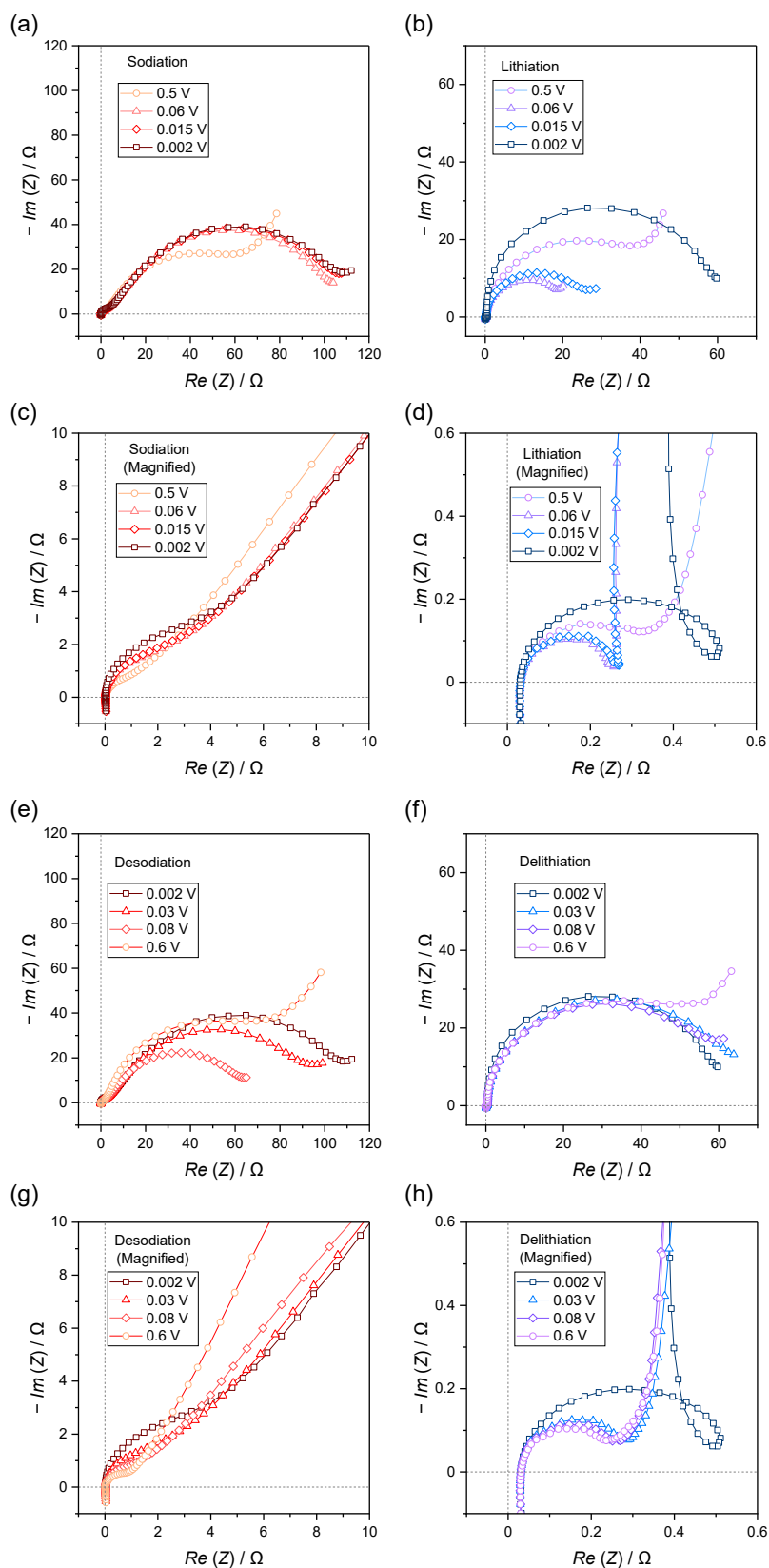


Figure S16. Nyquist plots of thick 40 vol.% HC-electrode in 3-electrodes cells. Electrode thickness were 65 μm and 74 μm for Na- and Li-cell, respectively. Impedance were measured from 1 MHz to 10 mHz during (a) sodiation, (b)lithiation, (c) desodiation, and (d) delithiation. High magnification of higher frequency region $> 1\text{Hz}$ during are shown in (e)–(h). Squidstat Plus (Admiral Instruments) was used as a potentiostat and an impedance analyzer.

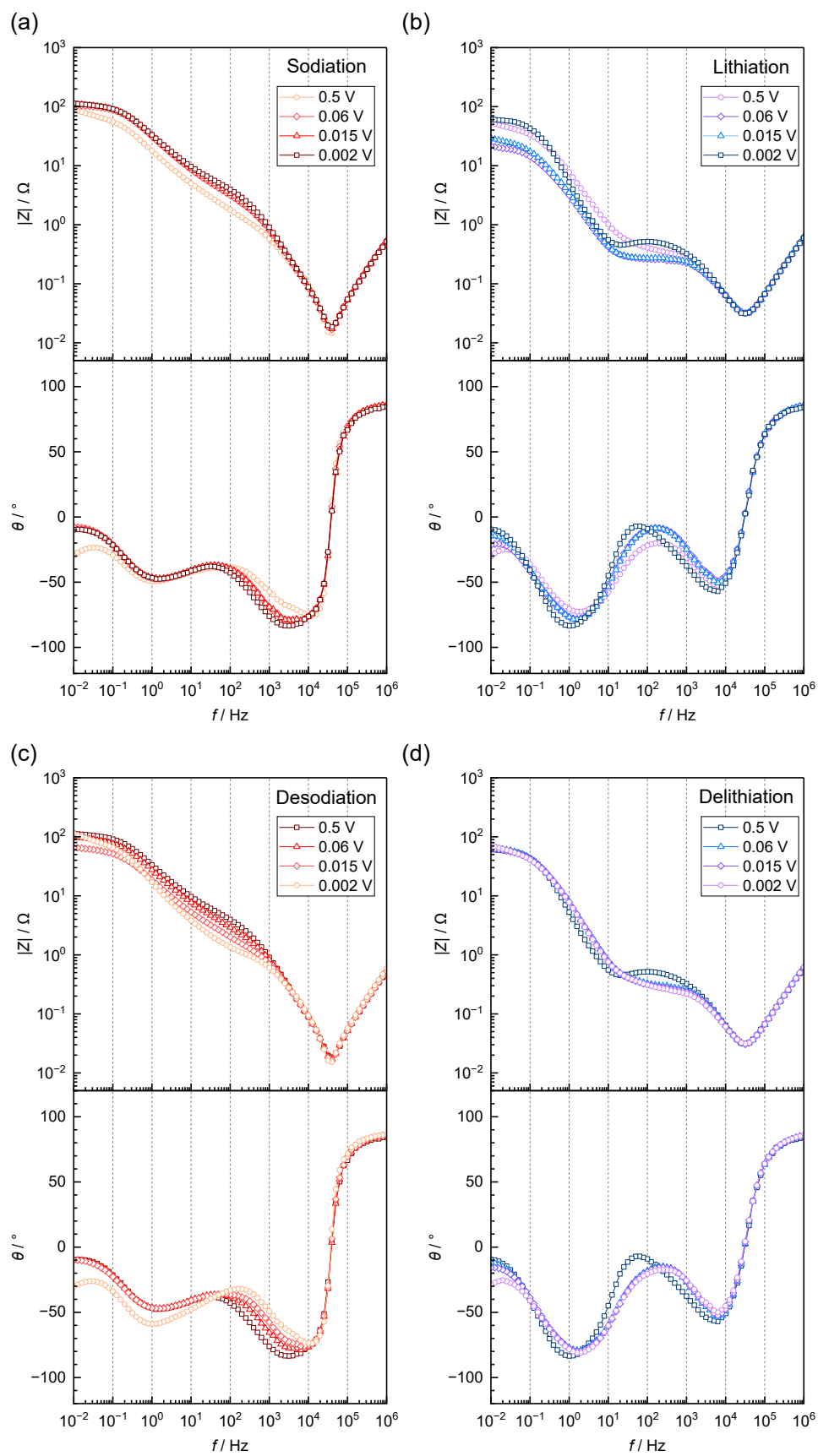


Figure S17. Bode plots of thick 40 vol.% HC-electrode in 3-electrodes cells during (a) sodiation, (b)lithiation, (c) desodiation, and (d) delithiation corresponding to Fig. S16.

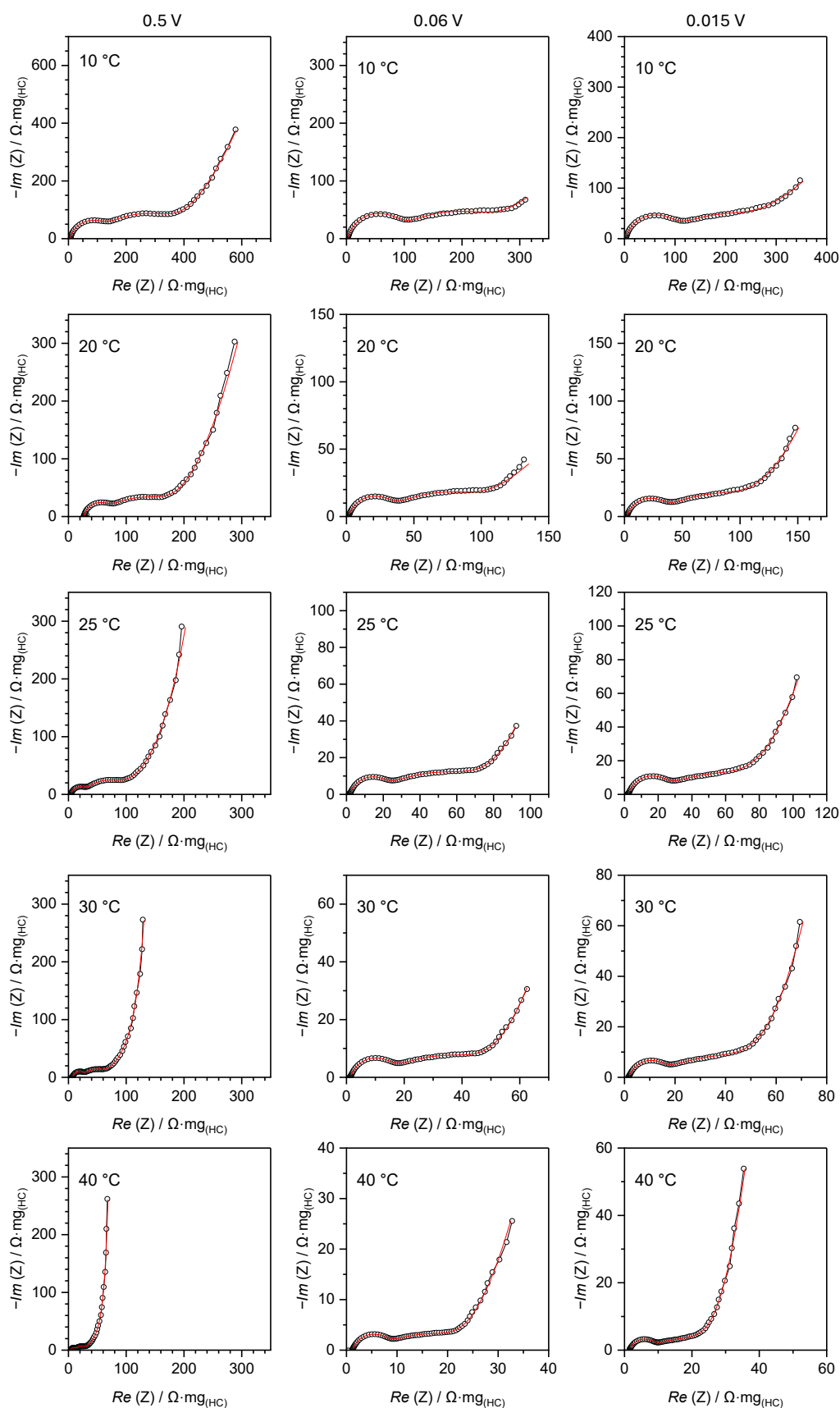


Figure S18. Nyquist plots of electrochemical impedance of 5 vol.% HC-electrode in Na-cell obtained after rate-capability tests. Graphs are aligned based on as testing temperature between 10–40 °C from top to bottom. Left, middle, and right column show results obtained at 0.5 V, 0.06 V, and 0.015 V, respectively.

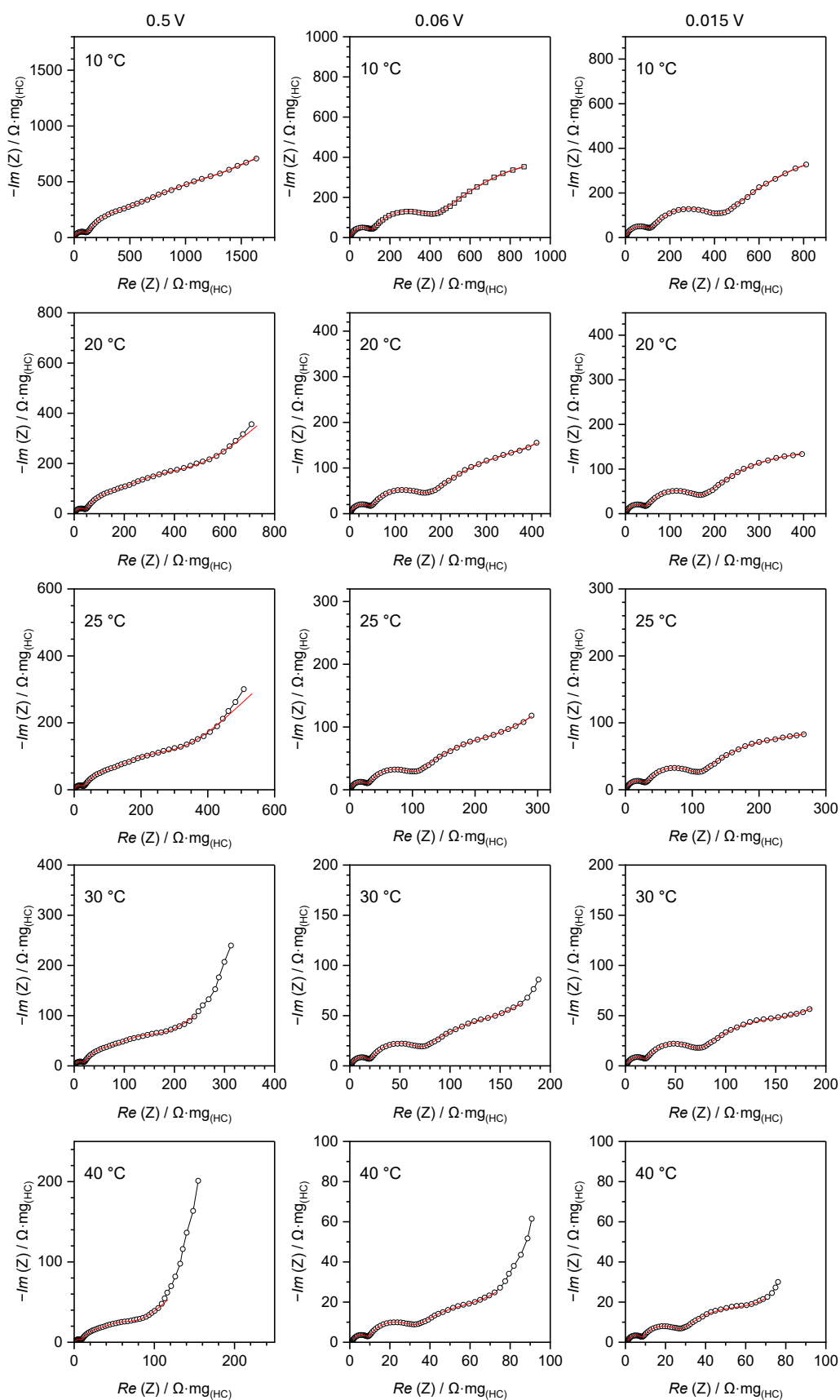
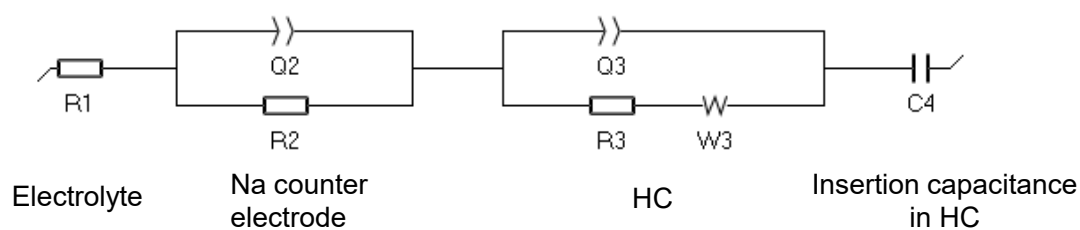


Figure S19. Nyquist plots of electrochemical impedance of 5 vol.% HC-electrode in Li-cell obtained after rate-capability tests. Graphs are aligned based on testing temperature between 10–40 °C from top to bottom. Left, middle, and right column show results obtained at 0.5 V, 0.06 V, and 0.015 V, respectively.

(a)



(b)

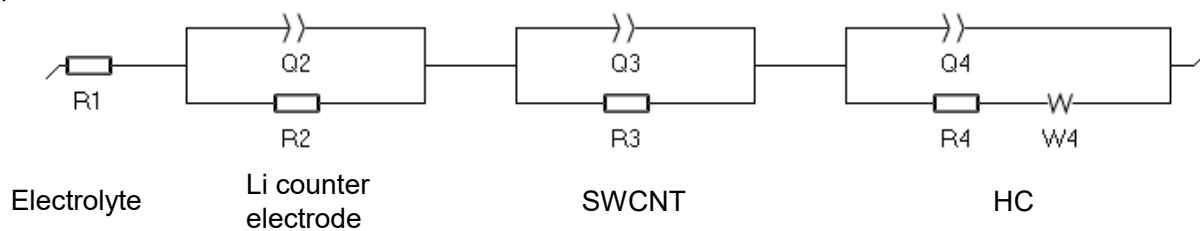


Figure S20. Equivalent circuits for EIS analysis applied to (a) Na cell and (b) Li cell. R3 in circuit (a) and R4 in circuit (b) are attributed to charge-transfer resistances. These equivalent circuit were prepared by referring to the study of single-particle electrodes.⁶

Table S4. R_{ct} of 5 vol. % HC-electrode in Na-/Li-cells extracted from Nyquist plots shown in Fig. S12 and S13. R_{ct} at 0.5 V

Temperature / °C	R_{ct} (Na) / $\Omega \cdot \text{mg}$	R_{ct} (Li) / $\Omega \cdot \text{mg}$
40	32	30
30	61	72
25	83	101
20	129	142
10	318	292

 R_{ct} at 0.06 V

Temperature / °C	R_{ct} (Na) / $\Omega \cdot \text{mg}$	R_{ct} (Li) / $\Omega \cdot \text{mg}$
40	17	23
30	39	50
25	61	74
20	93	116
10	223	290

 R_{ct} at 0.015 V

Temperature / °C	R_{ct} (Na) / $\Omega \cdot \text{mg}$	R_{ct} (Li) / $\Omega \cdot \text{mg}$
40	22	19
30	46	51
25	65	75
20	91	119
10	199	287

References in supporting information

1. K. Gotoh, M. Maeda, A. Nagai, A. Goto, M. Tansho, K. Hashi, T. Shimizu, and H. Ishida, "Properties of a novel hard-carbon optimized to large size Li ion secondary battery studied by ^7Li NMR" *Journal of Power Sources*, **162**, 1322 (2006).
2. Kureha Battery Materials Japan Co., Ltd., "High-performance Anode Material CARBOTRON® P" https://www.kureha.co.jp/development/story/pdf/catalog_hc_eg_20120924.pdf, (accessed 2023/04/30).
3. K. Kubota, S. Shimadzu, N. Yabuuchi, S. Tominaka, S. Shiraiishi, M. Abreu-Sepulveda, A. Manivannan, K. Gotoh, M. Fukunishi, M. Dahbi, and S. Komaba, "Structural Analysis of Sucrose-Derived Hard Carbon and Correlation with the Electrochemical Properties for Lithium, Sodium, and Potassium Insertion" *Chem. Mater.*, **32**, 2961 (2020).
4. H. Fujimoto, "A new estimation method for the degree of graphitization for random layer lattices" *Carbon*, **48**, 3446 (2010).
5. M. Okubo, Y. Tanaka, H. Zhou, T. Kudo, and I. Honma, "Determination of Activation Energy for Li Ion Diffusion in Electrodes" *J. Phys. Chem. B*, **113**, 2840 (2009).
6. K. Dokko, Y. Fujita, M. Mohamedi, M. Umeda, I. Uchida, and J. R. Selmán, "Electrochemical impedance study of Li-ion insertion into mesocarbon microbead single particle electrode: Part II. Disordered carbon" *Electrochimica Acta*, **47**, 933 (2001).